Effects of Bcl-2 Levels on Fas Signaling-Induced Caspase-3 Activation: Molecular Genetic Tests of Computational Model Predictions[1]

Fei Hua,[2]* Melanie G. Cornejo,* Michael H. Cardone,[‡] Cynthia L. Stokes,[§] and Douglas A. Lauffenburger*[†]

Fas-induced apoptosis is a critical process for normal immune system development and function. Although many molecular components in the Fas signaling pathway have been identified, a systematic understanding of how they work together to determine network dynamics and apoptosis itself has remained elusive. To address this, we generated a computational model for interpreting and predicting effects of pathway component properties. The model integrates current information concerning the signaling network downstream of Fas activation, through both type I and type II pathways, until activation of caspase-3. Unknown parameter values in the model were estimated using experimental data obtained from human Jurkat T cells. To elucidate critical signaling network properties, we examined the effects of altering the level of Bcl-2 on the kinetics of caspase-3 activation, using both overexpression and knockdown in the model and experimentally. Overexpression was used to distinguish among alternative hypotheses for inhibitory binding interactions of Bcl-2 with various components in the mitochondrial pathway. In comparing model simulations with experimental results, we find the best agreement when Bcl-2 blocks the release of cytochrome *c* by binding to both Bax and truncated Bid instead of Bax, truncated Bid, or Bid alone. Moreover, although Bcl-2 overexpression strongly reduces caspase-3 activation, Bcl-2 knockdown has a negligible effect, demonstrating a general model finding that varying the expression levels of signal molecules frequently has asymmetric effects on the outcome. Finally, we demonstrate that the relative dominance of type I vs type II pathways can be switched by varying particular signaling component levels without changing network structure. *The Journal of Immunology,* **2005, 175: 985–995.**

Apoptosis is an essential cellular event for maintaining homeostasis of the immune system and its normal function. Dysregulation of apoptosis can contribute to various autoimmune diseases and cancer (1, 2). One major mechanism for inducing apoptosis is through the activation of death receptors such as TNF, Fas (Apo-1/CD95), DR3 (TRAMP), DR4 (TRAIL-R1), and DR5 (TRAIL-R2) (3, 4). Among death receptors, the signaling pathways for Fas-induced apoptosis are the best characterized (5) (Fig. 1). Two pathways activated by Fas have been identified (6), and are referred to as type I and type II pathways. For both pathways, caspases, a family of cysteine proteases, are crucial for both the initiation and execution of apoptosis. The pathways diverge after activation of initiator caspases (e.g., caspase-8 and caspase-10) and converge at the end by activating executor caspases (e.g., caspase-3). In the type I pathway, initiator caspases cleave and activate executor caspases directly. In the type II pathway, also called the mitochondrial pathway, a more complex signaling cascade is activated involving the disruption of mitochondrial membrane potential. Fas signaling is tightly regulated at multiple steps along both signaling cascades (2, 4, 5, 7). For instance, FLIP blocks activation of initiator caspases, Bcl-2 prevents mitochondrial disruption, and X-linked inhibitor of apoptosis protein (XIAP)[3] inhibits downstream caspases (i.e., caspase-9 and caspase-3).

Despite the characterization of the components of these apoptotic pathways, we have an incomplete understanding of how all of the signaling molecules fit together into a single coherent network, and how the quantitative and dynamic aspects of the network function in relation to the final cellular outcome (i.e., apoptosis vs survival). Studies in other systems, such as the epidermal growth factor receptor (8), have shown that using computational models to study the dynamic behavior of an integrated signaling system can contribute significantly to understanding complex biological processes. In this study, we organize biochemical and biophysical knowledge about the Fas signaling pathway into a mechanistic mathematical model to advance our understanding of the integrative operation of this pathway. The model includes the components and behaviors of the signal transduction process from receptor binding to caspase-3 activation.

We first use model simulations with experiments to explore how the protein Bcl-2 regulates Fas signaling. Bcl-2 has been found to be a potent inhibitor of apoptosis in response to a variety of cytotoxic stimuli. It inhibits apoptosis through the mitochondrial pathway by preventing disruption of the mitochondria and the subsequent release of cytochrome *c*. Consequently, overexpression of Bcl-2 has a protective effect against Fas-induced apoptosis in cells

*Center for Cancer Research and [†]Biological Engineering Division, Massachusetts Institute of Technology, Cambridge, MA 02139; [‡]Merrimack Pharmaceuticals, Cambridge, MA 02142; and [§]Entelos, Foster City, CA 94404

Received for publication February 14, 2005. Accepted for publication May 3, 2005.

The costs of publication of this article were defrayed in part by the payment of page charges. This article must therefore be hereby marked *advertisement* in accordance with 18 U.S.C. Section 1734 solely to indicate this fact.

[1] This work was partially supported by Entelos, and the National Institute of General Medical Sciences Cell Decision Processes Center at Massachusetts Institute of Technology.

[2] Address correspondence to Dr. Fei Hua, Building 56, Room 353, Massachusetts Institute of Technology, 77 Massachusetts Avenue, Cambridge, MA 02139. E-mail address: fhua@mit.edu

[3] Abbreviations used in this paper: XIAP, X-linked inhibitor of apoptosis protein; tBid, truncated Bid; FasL, Fas ligand; PI, propidium iodide; FADD, Fas-associated death domain; DISC, death-inducing signaling complex; Smac, second mitochondria-derived activator of caspase; ODE, ordinary differential equation.

0022-1767/05/$02.00

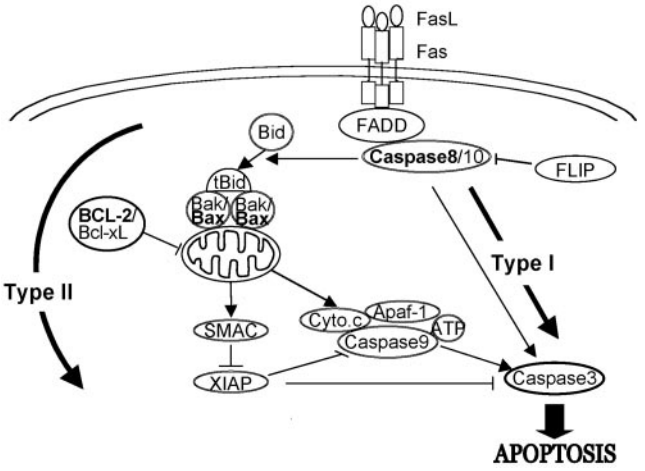

FIGURE 1. Schematic representation of the Fas signaling pathway. Molecules in bold are used in the model to represent two or more molecules with similar functions.

in which the type II pathway is dominant, but not in cells in which the type I pathway is dominant (6). However, the exact mechanisms by which Bcl-2 protects the mitochondrial pathway are not clear. Conflicting results have shown that Bcl-2 may or may not interact with Bid, truncated Bid (tBid), Bax, and Bak (9–12). This question could be approached experimentally using coimmunoprecipitation to observe which molecules coprecipitate with Bcl-2, or by staining multiple molecules to look for colocalization with microscopy techniques. However, both experimental methods can give ambiguous results due to their intricate nature, and they are limited by the lack of good Abs against tBid. Furthermore, neither approach is able to capture transient protein-protein interactions.

In this study, we use our Fas signaling model to explore four potential Bcl-2 mechanisms of action: Bcl-2 binding to Bax, Bid, or tBid individually, or both Bax and tBid. By examining the dynamic behavior of the system, the model suggests a simple experiment to differentiate the four hypotheses. Combining our model predictions with the experimental measurements, we discern that Bcl-2 interaction with both Bax and tBid is the most likely, as well as the most efficient, mechanism for Bcl-2 to block the mitochondrial pathway. Analysis of the model also suggests an explanation for potential insensitivity to Bcl-2 down-regulation.

In addition, we analyze how the model output for caspase-3 activation depends on signaling molecule levels to gain insight into the overall regulation of the Fas signaling pathway. The results show a prevalent phenomenon where increasing or decreasing the level of a molecule can have an asymmetrical effect on signaling outcome. Finally, we demonstrate that our model is capable of switching from the type II pathway dominant behavior (sensitive to Bcl-2 up-regulation) to the type I pathway dominant behavior (insensitive to Bcl-2 up-regulation) by simply increasing the level of caspase-8, while keeping the network structure unchanged.

Materials and Methods

Cells and reagents

Human tumor T cell line, Jurkat.E6, was purchased from American Type Culture Collection. Recombinant human SuperFasL was purchased from Alexis. For Western blot, rabbit anti-Bcl-2 polyclonal Ab was purchased from R&D Systems; rabbit anti-caspase-3 mAb was purchased from Santa Cruz Biotechnology; anti-tubulin mAb was obtained from Sigma-Aldrich. HRP-conjugated secondary Ab anti-mouse and anti-rabbit were purchased from Santa Cruz Biotechnology. PE-conjugated anti-Bcl-2 mAb (556536) and anti-active caspase-3 mAb (559565) used for intracellular staining were both purchased from BD Pharmingen. Fluor 647-conjugated anti-rabbit IgG Ab (A31573) was purchased from Molecular Probes.

Quantitative Western blot analysis

Resting or Fas ligand (FasL)-stimulated cells were washed once with ice-cold PBS, then lysed as described previously (13). Lysates from same number of cells were loaded in each lane. Proteins were separated on 12% polyacrylamide gel, then transferred to a polyvinylidene difluoride membrane. The reactive bands were detected by chemiluminescence (PerkinElmer) and captured with Kodak Image Station (Kodak). Band density was quantified using a Kodak 1D Image Analysis Software (Kodak). The linearity of the chemiluminescent signal was tested by a serial dilution of lysates. Measurements were always done within the linear range of the signal.

Intracellular staining of cleaved caspase-3 and Bcl-2

Resting or stimulated cells were fixed with 4% paraformaldehyde for 10 min at room temperature, followed by permeabilization with 100% MeOH overnight at −20°C. Cells were washed twice with PBS + 0.1% Tween (PBST) before incubating with anti-active caspase-3 (BD Pharmingen) for 1 h. Cells were washed twice again with PBST, then incubated with Fluor 647-conjugated anti-rabbit and PE-conjugated anti-Bcl-2 mAb at room temperature for 1 h in the dark. After two more washes with PBST, cells were analyzed on a FACSCalibur machine (BD Biosciences). For experiments to differentiate low and high amounts of Bcl-2 expression, cells were first gated on the level of Bcl-2, then gated on active caspase-3. The percentage of cells negative in active caspase-3 (i.e., percentage of cells with full-length caspase-3) were measured and normalized using the following formula: (percentage of cells negative in active caspase-3 with stimulation)/(percentage of cells negative in active caspase-3 without stimulation).

Cytotoxicity assay

Cells at density of 1×10^6 cells/ml were incubated in the culture medium with different concentrations of FasL in 96-well plates for 24 h. Cells were washed once with ice-cold PBS and resuspended in 5 μg/ml propidium iodide (PI), after which cells were immediately analyzed on a FACScan machine (BD Biosciences). Specific cell death was calculated using the formula: (percentage of total cell death − percentage of spontaneous death)/(100% − percentage of spontaneous death), where percentage of spontaneous death is the percentage of cell death without adding any stimulation.

Genetic manipulations

Stably transduced cell lines were generated as described previously (14, 15). Briefly, the Ca^{2+} precipitation method was used to transfect 293T cells. Supernatants collected 48 and 72 h after transfection were used to infect Jurkat cells. To overexpress Bcl-2, the MIG-Bcl2 vector was cotransfected with CMV-gag/pol and VSVG packaging vectors (15). To down-regulate Bcl-2, a short hairpin RNA sequence was selected and cloned into pll3.7 vector (14). The targeting sequence for Bcl-2 short hairpin RNA is GTGATGAAGTACATCCATT. pll3.7-Bcl2 was cotransfected with VSVG, RSV-REV, and pMDL g/p RRE. Empty MIG or pll3.7 vector was used as a control, respectively. Because both MIG and pll3.7 vectors contain enhanced GFP reporter gene, successfully infected cells were identified with green fluorescence. GFP-positive populations were sorted using FACStarPlus (BD Biosciences), and only the sorted cells were used for experiments.

Mathematical model

Model structure. A schematic representation of the Fas signaling network described by our computational model is shown in Fig. 1. The model starts with FasL binding to Fas and concludes at caspase-3 activation because the latter results in the cleavage of many important cellular substrates, leading to morphological changes that are typically associated with apoptosis. In the model, both Fas and FasL are preassociated as trimers (16, 17). Once FasL binds to Fas, the complex recruits Fas-associated death domain (FADD), which then recruits caspase-8, forming a death-inducing signaling complex (DISC) (18). Because the stoichiometry and type of molecular interactions at the DISC are not clear, we assumed 1:1 noncooperative interactions between Fas and FADD, and between FADD and caspase-8, with up to three FADD and three caspase-8 molecules recruited to the DISC. When two (or more) caspase-8 molecules are recruited to the DISC, they cleave each other, generating an intermediate cleavage product p43/41, which further cleaves itself to generate activated caspase-8. Although caspase-10 can also be recruited to the DISC and may have redundant

function with caspase-8, caspase-8 is included in our model as a functional surrogate for the combined effect.

Activated caspase-8 either cleaves and activates caspase-3 directly (type I pathway) or cleaves Bid into tBid to initialize the type II pathway. tBid recruits two Bax molecules, which leads to the release of cytochrome *c* and second mitochondria-activator of caspase (Smac) from the mitochondria. Bak and Bax have been shown to be redundant in tBid-induced cytochrome *c* release (19); therefore, we use Bax in the model to represent the combined functionality of both molecules. Subsequently, cytochrome *c* binds to Apaf-1 and two caspase-9 molecules in the presence of ATP, forming the apoptosome. Caspase-9 becomes activated in the apoptosome and then activates caspase-3. Smac released from the mitochondria can bind to XIAP. Several IAP molecules (XIAP, cIAP-1, cIAP-2) have been implicated in the regulation of apoptosis. We selected XIAP to represent the functionality of the IAP family because it has the highest binding affinity to caspases (20).

There are three negative regulators in this model: FLIP, Bcl-2, and XIAP. FLIP competes with caspase-8 to bind FADD, thereby preventing caspase-8 activation and inhibiting both the type I and II pathways. Bcl-2 in the model represents the net functionality of both Bcl-2 and Bcl-x_L, and functions to inhibit the type II pathway. The molecular mechanism by which Bcl-2 exerts this effect is unclear, and four separate hypotheses were analyzed. The initial model has Bcl-2 binding to Bax only. Alternative models include Bcl-2 binding to Bid alone, tBid alone, or Bax plus tBid. XIAP, the third negative regulator binds to both caspase-9 and active caspase-3 (20).

Model simulation. The model describing the signal transduction of the Fas pathway was created using Entelos PhysioLab Modeler (Entelos). Biochemical reactions were used to describe the molecular interactions. Most of the interactions were described with the following class of mass-action equation:

$$A + B \underset{k_r}{\overset{k_f}{\rightleftarrows}} C \tag{1}$$

where k_f is forward rate constant and k_r is reverse rate constant. Concentration changes of all the molecules were described by ordinary differential equations (ODEs):

$$\frac{dA}{dt} = \frac{dB}{dt} = -\frac{dC}{dt} = k_f \cdot A \cdot B - k_r \cdot C \tag{2}$$

Enzymatic reactions were split into two reactions, with k_f of the second one being 0:

$$S + E \leftrightarrow SE \rightarrow P + E \begin{cases} S + E \underset{k_r}{\overset{k_f}{\leftrightarrow}} SE \\ P + E \underset{k_{cat}}{\overset{}{\longleftarrow}} SE \end{cases} \tag{3}$$

The equations for Smac and cytochrome *c* release are different to represent transport processes, where the release of molecules depends on the amount of oligomerized Bax, but does not bind to oligomerized Bax:

$$A \xrightarrow{k_f \cdot B} A^* \tag{4}$$

where *A* is either the concentration of Smac or cytochrome *c* in mitochondria, *A** is the concentration of the same molecule in cytosol, and B is the concentration of oligomerized Bax. It is an irreversible reaction, and the concentration changes were described by the following ODEs:

$$\frac{dA}{dt} = -\frac{dA^*}{dt} = k_f \cdot A \cdot B \tag{5}$$

All the equations used in the model are listed in Table I. Fig. 2 is a graphical representation of all the biochemical reactions used for the model with Bcl-2 binding to Bax only.

Given the initial conditions (concentrations of molecules that are not zero before simulation starts, including the concentration of FasL) and the rate constants, Entelos PhysioLab Modeler solves all the ODEs numerically using a Runga-Kutta 5(4) adaptive step-size method and calculates concentration changes for all the molecules over time. There are 136 rate constants and 15 initial conditions in the model. Of the 136 rate constants, there are only 35 independent values because many of them were set to be the same, such as rate constants for caspase-8 or FLIP binding to FADD for different intermediate steps during DISC formation. The assumption of equal values in such cases was because we chose noncooperative binding for simplest reaction representations, in the absence of data indicating more complicated kinetics. There are 70 intermediate complexes with concentrations starting at zero.

Parameter estimation and model evaluation with experimentally measured kinetic data. Approximately one-third of the parameter values (rate constants and initial conditions) used in the model were taken from the literature or obtained through unpublished observations (Tables II and III). The remaining parameters were manually adjusted within an expected physiological range so that the model reproduced the behavior of Jurkat cells in the presence of 100 ng/ml FasL. More specifically, forward rate constants were limited to the range between 1×10^{-6} and 1×10^{-1} (diffusion limit) $nM^{-1}s^{-1}$; reverse rate constants were limited to 1×10^{-5} to $10\ s^{-1}$. The data used to tune the model were time-dependent reductions of caspase-8 and caspase-3 measured from Jurkat cells using quantitative Western blot assay (Fig. 3). The mean values of three experiments were used for model fitting. As seen in Fig. 3, *C* and *D*, the model can accurately represent the dynamics of both an upstream (caspase-8) and a downstream (caspase-3) signal in response to FasL stimulation. All the resulting rate constants are listed in Table II, and the initial conditions are listed in Table III. These values are referred to as baseline values.

The values of cellular protein levels obtained from most experimental methods typically represent means across a cell population, whereas any individual cell within the population may possess a set of values different from the means but within heterogeneous distributions around those means. To test whether the averaged behavior of diverse cells across a population is similar to a representative cell possessing the set of population-averaged values for all the parameters, we undertook Monte Carlo simulations of many diverse individual cells possessing sets of parameter values randomly selected from within normal distributions around the means (using SDs expected from typical Western blot measurements). The averaged behavior of these cells, in terms of their dynamic caspase-8 and caspase-3 activations, from this set of simulations were sufficiently close to the result from the representative cell possessing the mean parameter values (results not shown). Therefore, in this particular model, we believe that we can use the representative cell with mean parameters satisfactorily.

Results

Bcl-2 blocks the mitochondrial pathway by binding to both tBid and Bax/Bak

Bcl-2 is known to block the mitochondrial pathway; however, the exact mechanism by which Bcl-2 exerts its effect is still not clear. Our model is adjusted to describe the Fas signaling pathway in Jurkat cells, which are known to be sensitive to the overexpression of Bcl-2 (6, 21). Therefore, we could use this model to explore how different mechanisms of Bcl-2 blockage of the mitochondrial pathway may generate different dynamics of caspase-3 activation.

In our initial model, Bcl-2 binds to Bax; however, there are suggestions in the literature that Bcl-2 may bind to only Bid, only tBid, or both Bax and tBid (9–12). To test these different hypotheses, we generated three new models, changing only the specific molecule interacting with Bcl-2. The initial concentration of Bcl-2, as well as the association and dissociation rate constants for Bcl-2 interacting with other molecules, was kept the same in all four models. For 100 ng/ml FasL stimulation, the four models show very similar kinetics of caspase-3 activation when Bcl-2 is at the baseline value (Fig. 4*A*). In contrast, when the Bcl-2 level is increased by 10 or 100 times (simulating its overexpression), caspase-3 activation kinetics are quite different for the four models (Fig. 4, *B–E*). The model with Bcl-2 binding to both Bax and tBid is the most sensitive to increases in Bcl-2, where only a 10-fold increase of Bcl-2 almost completely blocks the mitochondrial pathway (Fig. 4*E*). On the other hand, the model with Bcl-2 binding to Bax alone is somewhat less sensitive to Bcl-2 overexpression (Fig. 4*B*), whereas the model with Bcl-2 binding to Bid alone is the least sensitive (Fig. 4*C*). Because the effect of Bcl-2 binding to Bid is minimal, the model with Bcl-2 binding to both Bax and

Table I. *Biochemical reactions*

Reactant A[a]	Reactant B	Reactant C	Forward Reaction Rate	Reverse Reaction Rate	Comment
FasL	Fas	FasC	k1_f	k1_r	
FasC	FADD	FasC:FADD	k2_f	k2_r	Assume noncooperative binding between FADD and Fas, which means that regardless of other molecules in the complex, the FADD-Fas interaction always has the same rate constant.
FasC:FADD	FADD	FasC:FADD_2	k2_f	k2_r	
FasC:FADD_2	FADD	FasC:FADD_3	k2_f	k2_r	
FasC:FADD_2:Casp8	FADD	FasC:FADD_3:Casp8	k2_f	k2_r	
FasC:FADD_2:FLIP	FADD	FasC:FADD_3:FLIP	k2_f	k2_r	
FasC:FADD_2:Casp8_2	FADD	FasC:FADD_3:Casp8_2	k2_f	k2_r	
FasC:FADD_2:Casp8:FLIP	FADD	FasC:FADD_3:Casp8:FLIP	k2_f	k2_r	
FasC:FADD_2:FLIP_2	FADD	FasC:FADD_3:FLIP_2	k2_f	k2_r	
FasC:FADD:Casp8	FADD	FasC:FADD_2:Casp8	k2_f	k2_r	
FasC:FADD:FLIP	FADD	FasC:FADD_2:FLIP	k2_f	k2_r	
FasC:FADD_3	Casp8	FasC:FADD_3:Casp8	k3_f	k3_r	Assume caspase-8 and FLIP have the same binding rate constants for FADD, because their death effector domains (FADD binding domain) have high homology (38).
FasC:FADD_3	FLIP	FasC:FADD_3:FLIP	k3_f	k3_r	
FasC:FADD_3:Casp8	Casp8	FasC:FADD_3:Casp8_2	k3_f	k3_r	
FasC:FADD_3:Casp8	FLIP	FasC:FADD_3:Casp8_FLIP	k3_f	k3_r	
FasC:FADD_3:FLIP	Casp8	FasC:FADD_3:Casp8:FLIP	k3_f	k3_r	Similar to binding between FADD and Fas, assume noncooperative binding between FADD and caspase-8 and between FADD and FLIP.
FasC:FADD_3:FLIP	FLIP	FasC:FADD_3:FLIP_2	k3_f	k3_r	
FasC:FADD_3:Casp8_2	Casp8	FasC:FADD_3:Casp8_3	k3_f	k3_r	
FasC:FADD_3:Casp8_2	FLIP	FasC:FADD_3:Casp8_2:FLIP	k3_f	k3_r	
FasC:FADD_3:Casp8:FLIP	Casp8	FasC:FADD_3:Casp8_2:FLIP	k3_f	k3_r	
FasC:FADD_3:Casp8:FLIP	FLIP	FasC:FADD_3:Casp8:FLIP_2	k3_f	k3_r	
FasC:FADD3:FLIP_2	Casp8	FasC:FADD_3:Casp8:FLIP_2	k3_f	k3_r	
FasC:FADD_3:FLIP_2	FLIP	FasC:FADD_3:FLIP_3	k3_f	k3_r	
FasC:FADD_2	Casp8	FasC:FADD_2:Casp8	k3_f	k3_r	
FasC:FADD_2	FLIP	FasC:FADD_2:FLIP	k3_f	k3_r	
FasC:FADD_2:Casp8	Casp8	FasC:FADD_2:Casp8_2	k3_f	k3_r	
FasC:FADD_2:Casp8	FLIP	FasC:FADD_2:Casp8:FLIP	k3_f	k3_r	
FasC:FADD_2:FLIP	Casp8	FasC:FADD_2:Casp8:FLIP	k3_f	k3_r	
FasC:FADD_2:FLIP	FLIP	FasC:FADD_2:FLIP_2	k3_f	k3_r	
FasC:FADD	Casp8	FasC:FADD:Casp8	k3_f	k3_r	
FasC:FADD	FLIP	FasC:FADD:FLIP	k3_f	k3_r	
FasC:FADD_2	Casp8_2_p41	FasC:FADD-2:Casp8_2		k4	
FasC:FADD_3:Casp8	Casp8_2_p41	FasC:FADD-3:Casp8_3		k4	
FasC:FADD_3:FLIP	Casp8_2_p41	FasC:FADD-3:Casp8_2:FLIP		k4	
FasC:FADD_3	Casp8_2_p41	FasC:FADD-3:Casp8_2		k4	
Casp8_2_p41		Casp8_2*	k5		Nongeneral reaction: $A \xrightarrow{k_f} A^*$
Casp8_2*	Casp3	Casp8_2*:Casp3	k6_f	k6_r	
Casp8_2*	Casp3*	Casp8_2*:Casp3		k7	Assume the catalytic reaction rate of caspase_8 is the same regardless of the substrate.
Casp8_2*	tBid	Cas8_2*:Bid		k7	
Casp8_2*	Bid	Cas8_2*:Bid	k8_f	k8_r	
tBid	Bax	tBid:Bax	k9_f	k9_r	Assume the first Bax and the second Bax binding to tBid have the same rate constants.
tBid:Bax	Bax	tBid:Bax_2	k9_f	k9_r	
Smac	Bax	Smac*	k10		Assume Smac and Cyto.*c* have the same release rate.
Cyto.*c*	Bax	Cyto.*c**	k10		Nongeneral reaction: $A \xrightarrow{k_f \cdot B} A^*$
Smac*	XIAP	Smac*:XIAP	k11_f	k11_r	
Cyto.*c**	Apaf	Cyto.*c**:Apaf:ATP	k12_f	k12_r	Nongeneral reaction: $A + B + ATP \underset{k_r}{\overset{k_f}{\rightleftharpoons}} C$
Cyto.*c**:Apaf:ATP	Casp9	Cyto.*c**:Apaf:ATP:Casp9	k13_f	k13_r	
Cyto.*c**:Apaf:ATP:Casp9	Casp9	Cyto.*c**:Apaf:ATP:Casp9_2	k14_f	k14_r	
Cyto.*c**:Apaf:ATP:Casp9	Casp9*	Cyto.*c**:Apaf:ATP:Casp9_2		k15	
Casp9*	Casp3	Casp9*:Casp3	k16_f	k16_r	

(*Table continues*)

Table I. *Continued*

Reactant A[a]	Reactant B	Reactant C	Forward Reaction Rate	Reverse Reaction Rate	Comment
Casp9*	Casp3*	Casp9*:Casp3		k17	
Casp9	XIAP	Casp9:XIAP	k18_f	k18_r	
Casp3*	XIAP	Casp3*:XIAP	k19_f	k19_r	
Equations used for different models					
Bcl_2 binding to Bax alone					
Bcl_2	Bax	Bcl2:Bax	k20_f	k20_r	
Bcl_2 binding to Bid alone					
Bcl_2	Bid	Bcl2:Bid	k20_f	k20_r	
Bcl_2 binding to tBid alone					
Bcl_2	tBid	Bcl2:tBid	k20_f	k20_r	
Bcl_2 binding to both tBid and Bax					
Bcl_2	Bax	Bcl2:Bax	k20_f	k20_r	
Bcl_2	tBid	Bcl2:tBid	k20_f	k20_r	

[a] General reaction: $A + B \underset{k_r}{\overset{k_f}{\rightleftharpoons}} C$

Bid gives results similar to those observed when Bcl-2 binds to Bax alone (data not shown).

These simulation results indicate that the kinetic profile of caspase-3 activation in a cell line in which Bcl-2 is overexpressed could be used to distinguish between the four hypotheses about the mechanism of action of Bcl-2. Although Bcl-2 overexpression has been shown to protect Jurkat cells from Fas-induced apoptosis (6), the effect of Bcl-2 overexpression, especially different amounts of Bcl-2 overexpression, on the kinetics of caspase-3 activation in Jurkat cells has not been quantitatively measured. Therefore, we generated a stable, Bcl-2-overexpressing Jurkat cell line. In agreement with prior studies, Bcl-2 overexpression reduced the degree of apoptosis following stimulation by FasL (Fig. 5*A*). Intracellular staining for Bcl-2 shows a wide range of Bcl-2 up-regulation in the cell lines transduced with the MIG-Bcl-2 vector (wider peak) compared with a relatively uniform expression level (narrower peak) for the control cell line infected with the empty MIG vector (Fig. 5*B*). This wide range of Bcl-2 up-regulation allowed us to isolate subpopulations of cells with low and high levels of Bcl-2 overexpression. Using Bcl-2 and active caspase-3 double intracellular staining, kinetics of caspase-3 activation following stimulation with 100 ng/ml FasL was measured in these two subpopulations. Fig. 5*C* shows one representative experiment of three. The low Bcl-2 overexpressing subpopulation (mean fluorescence intensity, 74.4) had a mean intensity ~6 times that of the control cell line (mean fluorescence intensity, 12.6), whereas the high Bcl-2 overexpressing subpopulation (mean fluorescence intensity, 508) had a mean intensity ~50 times that of the control cell line (Fig. 5*B*). Caspase-3 activation is slowed in both subpopulations compared with control cells (Fig. 5*C*). In addition, there is neither a significant difference in the kinetics of caspase-3 activation between these two subpopulations, nor between them and the total heterogeneous Bcl-2-overexpressing population (Fig. 5*C*). These results show that a 6-fold increase of Bcl-2 expression is sufficient to reach a maximum level of inhibition. The residual caspase-3 activation is likely due to activation through the type I pathway. Comparison of these experimental results with simulation results from the four models (Fig. 4, *B–E*) supports the hypothesis that

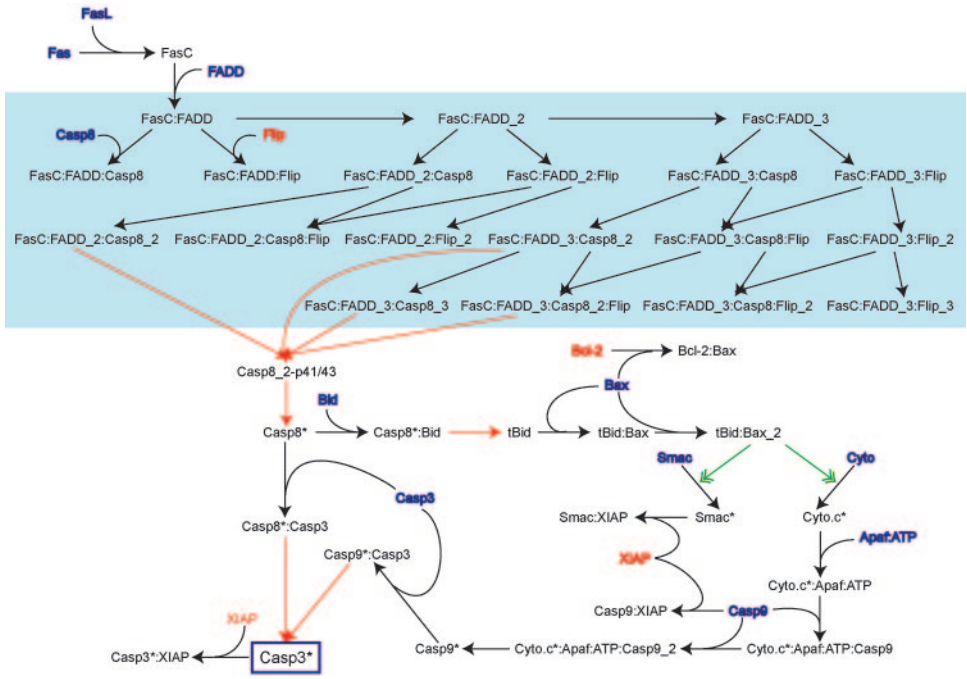

FIGURE 2. Translating the Fas signaling pathway into biochemical reactions in the model. Molecules in blue are directly involved in Fas signaling; molecules in red are negative regulators of the pathway; and molecules in black are transient intermediate complexes. Arrows in red represent catalytic reactions, and arrows in green represent transport processes as described in *Materials and Methods*. Blue shaded area encloses steps for DISC formation, where the molecule FLIP or caspase-8 is omitted for most reactions. The model is shown here with Bcl-2 binding to Bax only.

Table II. *Reaction rate constants*

Rate Constant	Value	Reference
k1_f	9.09E-05 $nM^{-1}s^{-1}$	K_d = *k1_r/k1_f* = 1.1 nM from (39)
k1_r	1.00E-04 s^{-1}	
k2_f	5.00E-04 $nM^{-1}s^{-1}$	
k2_r	0.2 s^{-1}	
k3_f	3.50E-03 $nM^{-1}s^{-1}$	
k3_r	0.018 s^{-1}	
k4	0.3 s^{-1}	
k5	0.1 s^{-1}	
k6_f	1.00E-05 $nM^{-1}s^{-1}$	
k6_r	0.06 s^{-1}	
k7	0.1 s^{-1}	
k8_f	5.00E-03 $nM^{-1}s^{-1}$	
k8_r	0.005 s^{-1}	
k9_f	2.00E-04 $nM^{-1}s^{-1}$	
k9_r	0.02 s^{-1}	
k10	1e-3 s^{-1}	
k11_f	7.00E-03 $nM^{-1}s^{-1}$	k_{on} = *k11_f* = 7e6/(M s) and k_{off} = *k11_r* = 2.21e-3/s from (40)
k11_r	2.21E-03 s^{-1}	
k12_f	2.78e-7 nM^{-1} $s^{-1}nM^{-1}$	
k12_r	5.70E-03 s^{-1}	
k13_f	2.84E-04 $nM^{-1}s^{-1}$	
k13_r	0.07493 s^{-1}	
k14_f	4.41E-04 $nM^{-1}s^{-1}$	
k14_r	0.1 s^{-1}	
k15	0.7 s^{-1}	
k16_f	1.96E-05 $nM^{-1}s^{-1}$	K_m = *(k16_r + k17)/k16_f* = 248 μM from (41)
k16_r	0.05707 s^{-1}	
k17	4.8 s^{-1}	k_{cat} = k17 = 4.8/s from (41)
k18_f	1.06E-04 $nM^{-1}s^{-1}$	K_i = *k18_r/k18_f* = 9.4e-9 M from (42)
k18_r	1.00E-03 s^{-1}	
k19_f	2.47E-03 $nM^{-1}s^{-1}$	k_{on} = *k19_f* = 2.5e6/(M s) and k_{off} = *k19_r* = 2.4e-3/s from (43)
k19_r	2.40E-03 s^{-1}	
k20_f	2.00E-03 $nM^{-1}s^{-1}$	K_d = *k20_r/k20_f* = 1e-8 M from (44)
k20_r	0.02 s^{-1}	

Table III. *Initial conditions*

Parameter	Value (nM)	Reference
Fas	10.00	
FasL	2.00	Equivalent to 100 ng/ml FasL
FADD	16.67	Unpublished observations
Flip	81.00	
Casp8	33.33	(45)
Casp3	200.00	(45)
Bid	25.00	
Bcl2	75.00	
Bax	83.33	
Cyto*c*	100.00	
Smac	100.00	
XIAP	30.00	(45)
Casp9	20.00	(41)
ATP	10.00	
Apaf	100.00	

Bcl-2 binds to both Bax and tBid to efficiently block the mitochondrial pathway.

Analysis of the reaction equations in the model helps explain why the kinetic differences among the models arise. In the models in which Bcl-2 binds to Bax alone (Fig. 4*B*) or to both Bax and tBid (Fig. 4*E*), some Bcl-2 preassociates (before Fas stimulation) with Bax through a reversible equilibrium reaction, with the potential (given enough preassociation) to block the type II pathway. The more Bcl-2 a cell has, the more Bax is bound by Bcl-2, and the blockade of the type II pathway is increased. At the same time, the amount of free Bcl-2 also increases. In the model with Bcl-2 interacting with both tBid and Bax, free Bcl-2 molecules are available to bind to tBid, and thus further block the type II pathway. Therefore, this mechanism gives the highest efficiency of blocking the mitochondrial pathway, whereas the mechanism of Bcl-2 binding to Bax alone gives the second highest efficiency. When Bcl-2 binds only Bid, the low sensitivity to Bcl-2 overexpression arises (Fig. 4*C*) because the binding between Bcl-2 and Bid is a reversible reaction, whereas Bid is irreversibly cleaved by active caspase-8 to generate tBid. Consequently, Bid can "escape" from Bcl-2 sequestration by being truncated by caspase-8 and continue the type II pathway activation. Theoretically, all Bid molecules can eventually be cleaved into tBid regardless of the concentration of Bcl-2, although the greater the Bcl-2 concentration, the slower the process. The model with Bcl-2 binding to tBid alone is also relatively insensitive to increases of Bcl-2 (Fig. 4*D*), although the binding reaction is reversible. This is because tBid is not formed until the signal cascade is initiated by FasL binding, and Bcl-2 and Bax must compete for tBid in reversible reactions. Even with stronger binding between Bcl-2 and tBid ($K_d = 10^{-8}$ M) than between Bax and tBid ($K_d = 10^{-7}$ M), the competition allows some tBid to associate with Bax and continue the signal transduction along the type II pathway.

Based on these findings, all further simulations were done using the model with Bcl-2 binding to both Bax and tBid.

Insensitivity of Fas-induced apoptosis to a decrease in Bcl-2 expression level

Aberrant Bcl-2 expression has been identified in many different cancers (22). Treatments aimed at decreasing the level of Bcl-2, such as Bcl-2 antisense drugs and small molecule inhibitors of Bcl-2, have been explored as anticancer agents (22, 23). We tested whether the model can predict the effect of decreasing Bcl-2 on caspase-3 activation. Surprisingly, whereas overexpressing Bcl-2 in Jurkat cells slows caspase-3 activation, reducing the level of Bcl-2 using the RNA interference technique in Jurkat cells (Fig. 6*A*) neither increases the sensitivity to Fas-induced apoptosis (Fig. 6*B*) nor accelerates caspase-3 activation (Fig. 6*C*). Consistent with this experimental data, decreasing Bcl-2 by 10- or 100-fold in the model has only a minimal effect on caspase-3 activation (Fig. 6*D*).

In the experiment, because the regulatory molecule Bcl-x_L is also known to block the mitochondrial pathway, it is possible that knocking down Bcl-2 has little effect on caspase-3 activation due to compensation from Bcl-x_L. In our model, Bcl-2 and Bcl-x_L were aggregated into a single entity we called "Bcl-2," so that under- or overexpression in the model represents a net decrease or increase of both molecules. Analysis of the model reveals that cells can be insensitive to the aggregated Bcl-2 molecule when their total level before reduction is relatively low, but not insignificant, allowing the type II pathway to be essentially "open." To start having an inhibitory effect on the type II pathway, Bcl-2/Bcl-x_L must not only be expressed, but also be expressed in excess of a threshold level, which is determined by a balance among Bcl-2, Bid, and Bax, and their reaction rate constants. Moreover, model analysis also suggests that a small amount of blockage of the signal transduction by Bcl-2 does not affect downstream caspase-3 activation because of the nonlinearity of the signal propagation. Although these model predictions need to be further tested by double knockdown of Bcl-2 and Bcl-x_L, the expression level of Bcl-x_L in Jurkat

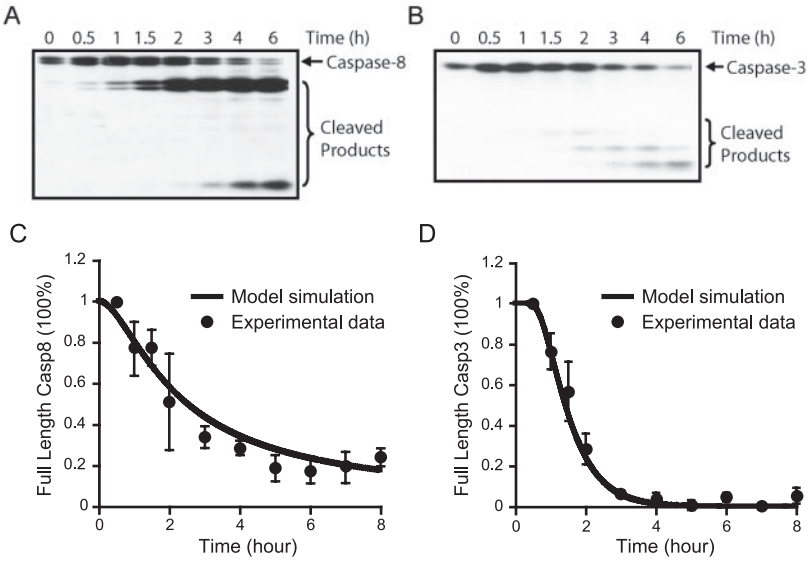

FIGURE 3. Model fitting. *A* and *B*, Representative Western blot showing the time course of caspase-8 (*A*) and caspase-3 (*B*) activation following stimulation of 100 ng/ml FasL in Jurkat cells. *C* and *D*, Good fit between model output and the experimental data for caspase-8 (*C*) and caspase-3 (*D*). The amount of full-length caspases averaged from three experiments was quantified and plotted vs time. Error bars represent SEM.

cells is relatively low compared with other cell types (data not shown), and no Bcl-x_L up-regulation was observed with Bcl-2 knockdown (Fig. 6*A*). Therefore, Bcl-x_L compensation may not be a confounding factor in our interpretation for Jurkat cells.

Asymmetrical effects of varying expression levels of the Fas signaling network components

Using a computational model to predict the effects of increasing or decreasing a single component in the model is a mathematical technique termed "sensitivity analysis." If perturbation of a given molecule has a relatively large impact on the outcome, the system is considered to be sensitive to the level of this molecule. In the above studies, we increased and decreased the Bcl-2 level in the model to discern its effects on caspase-3 activation. Our associated overexpression and knockdown experimental studies tested the veracity of those predictions.

We applied this analytical technique to all of the molecular components of the model except caspase-3 by varying the initial concentration of each molecule by one and two orders of magnitude higher and lower than the baseline values. The half-time for caspase-3 activation is used to represent how fast caspase-3 becomes activated (Fig. 7). The faster the full-length caspase-3

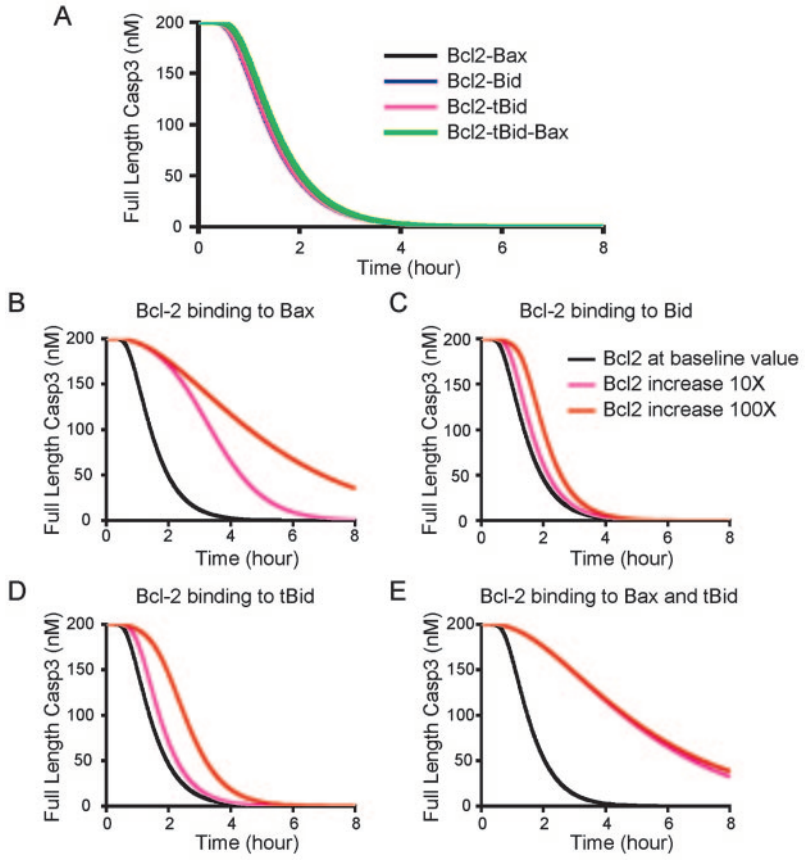

FIGURE 4. Sensitivity of caspase-3 activation to increases in Bcl-2 level. Four models were generated that differed only in the molecule(s) to which Bcl-2 binds. *A*, Comparison of caspase-3 activation among all four models with Bcl-2 level at the baseline value. *B–E*, Kinetics of caspase-3 activation with a baseline amount of Bcl-2, 10 or 100 times increased Bcl-2 levels from the model with Bcl-2 binding to Bax only (*B*), Bid only (*C*), tBid only (*D*), or both Bax and tBid (*E*).

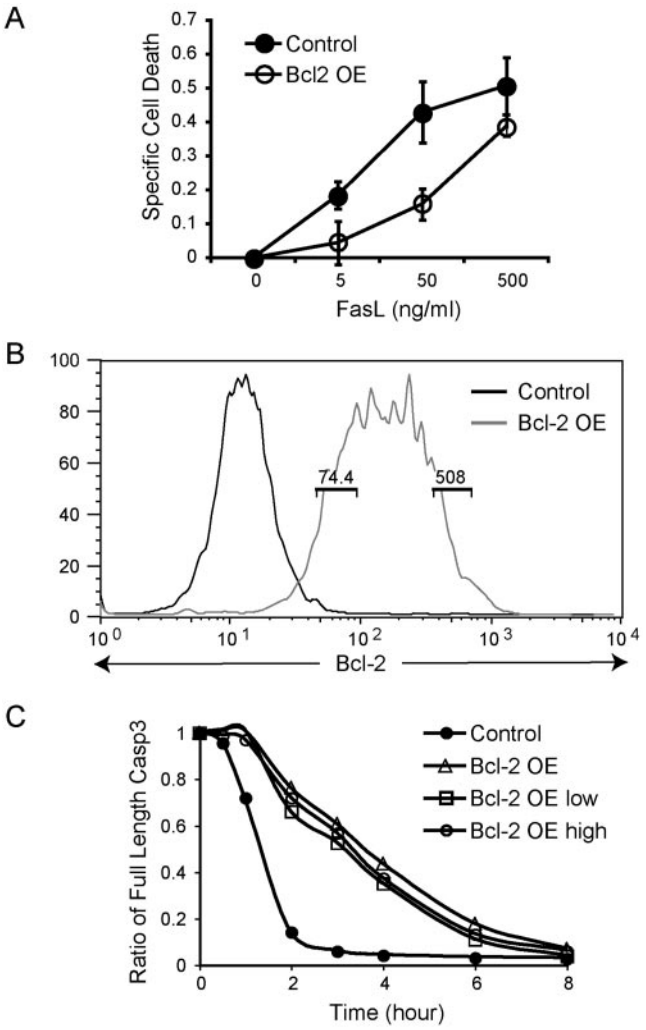

FIGURE 5. Effects of Bcl-2 overexpression on caspase-3 activation in Jurkat cells. *A*, Dose response to FasL-induced apoptosis in control cells transduced with empty MIG vector (●) or Bcl-2 overexpressing (OE) cells tranduced with MIG-Bcl-2 (○). Cells were incubated with the indicated concentration of FasL for 24 h, after which apoptosis was measured by PI staining. *B*, Intracellular staining of Bcl-2 in control and Bcl-2-overexpressing cells. The two gates on the FACS plot indicate the low and high Bcl-2-overexpressing subpopulations, with the average fluorescence intensity shown for each population. *C*, Time course of caspase-3 activation following stimulation with 100 ng/ml FasL. Active caspase-3 was measured by intracellular staining with flow cytometry in control cells (●), the whole population of Bcl-2-overexpressing cells (△), and subpopulations of low (□) and high (○) levels of Bcl-2-over-expressing-cells.

level decreases, the shorter the half-time is, and vice versa. As described above, caspase-3 activation has an asymmetric sensitivity to Bcl-2, being sensitive to increases of Bcl-2, but not to decreases of Bcl-2. Similar asymmetric sensitivities are observed for many molecules. For example, caspase-3 activation is sensitive to increases in the levels of FLIP and XIAP, but not to decreases in these molecules. Conversely, caspase-3 activation is sensitive to decreases, but not increases in the levels of Apaf-1, cytochrome *c*, FADD, and Bid. Caspase-3 activation is sensitive to changes in caspase-8 and caspase-9 in both directions. These results suggest that because changes in Bax, caspase-9, Bcl-2, and XIAP most dramatically block caspase-3 activation, these molecules could be good targets for blocking Fas signaling and reducing apoptosis in cells that function similar to Jurkat cells. Conversely, the analysis predicts that the only efficient way to increase apoptosis in Jurkat cells is to increase caspase-8 or caspase-9 levels.

Generating the type I pathway dominant behavior in the modified model

Human cells that are not sensitive to Bcl-2 overexpression have been identified in the literature (6, 24). In these cells, following FasL stimulation, caspase-3 is activated mostly through the type I pathway, such that even if the type II pathway is functioning normally in these cells, blocking it by Bcl-2 has only a minimal effect on caspase-3 activation. It has been suggested that the amount of active caspase-8 generated following FasL stimulation determines type I or type II dominancy (6, 24), reasoning that large amounts of activated caspase-8 can directly activate a sufficient amount of caspase-3 to induce death. In contrast, if only a small amount of caspase-8 is generated at the DISC, the type II pathway becomes essential to amplify the signal. To test this hypothesis in our model, we increased the formation of active caspase-8 by increasing the concentration of caspase-8 to 20 times the baseline value, while keeping everything else in the model unchanged (Fig. 8). This leads to faster caspase-3 activation kinetics (black line, compared to Fig. 4*A*). In addition, caspase-3 activation in this modified model becomes insensitive to a 100-fold increase in Bcl-2 (red line), which is the phenotype for the type I pathway dominant behavior. This consistency between the hypothesis and model simulation results both further validates the model and provides mechanistic validation for the hypothesis derived from experimental phenomenon.

Discussion

We developed a mathematical model describing Fas signaling that starts with FasL binding to Fas, ends at caspase-3 activation, and includes both type I and type II pathways. Our model of the Fas signaling pathway provides some additional useful characteristics and capabilities to those models that have been published previously (25, 26). In particular, our model integrates both the type I and type II pathways into an integrated signaling network so that, following Fas binding, the flux through each pathway is determined strictly by the reaction kinetics and signal molecule levels. This provides the ability to study the regulation of both pathways and the balance between them within an integrated system. We have used experimental data from the Jurkat cell line, a type II pathway dominant cell type, to calibrate our model structure and assign parameter values. This focus on the type II pathway provided the capability, with complementary experiments, to investigate the regulation of that pathway by the molecular component Bcl-2. In comparison, Fussenegger et al. (25) did not attempt to validate their model structure and parameter values against experimental data. Bentele et al. (26) used data from a type I pathway dominant cell type, a human B lymphoblastoid cell line, to adjust their model structure and parameter values, and consequently investigated the regulation of Fas signaling through the type I pathway, in particular the role of FLIP.

Mechanisms of Bcl-2 blocking the type II pathway

Bcl-2 has been a promising target molecule for anticancer therapies (27), and a better understanding of its function should help in the development of effective drugs targeting its regulation of the mitochondrial pathway. Combining model predictions with experiments, our results support the hypothesis that Bcl-2 inhibits the type II pathway by binding to both Bax and tBid, giving a strong antiapoptotic effect of Bcl-2 compared with the other scenarios tested.

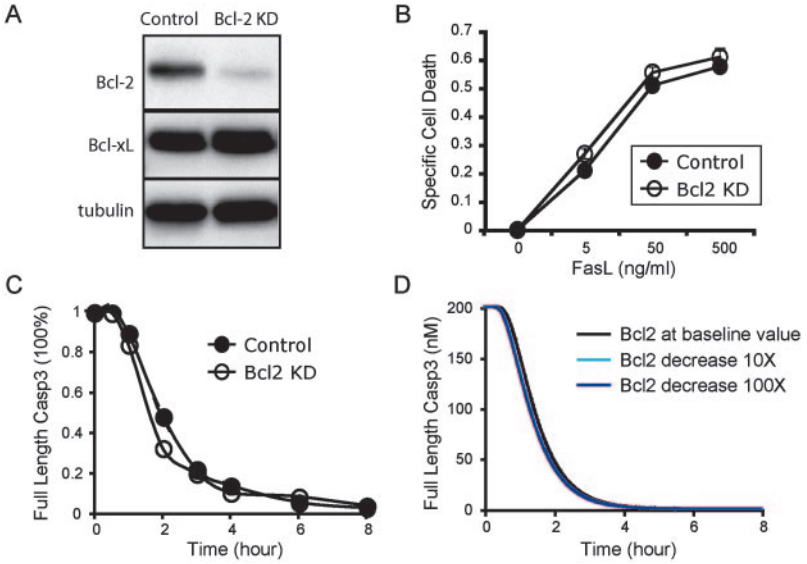

FIGURE 6. Insensitivity of caspase-3 activation to Bcl-2 down-regulation demonstrated by both experiments and computational simulation. *A*, Western blot analysis for Bcl-2 and Bcl-x_L in control cells transduced with empty pll3.7 vector or Bcl-2 knockdown (KD) cells tranduced with pll3.7-Bcl-2. Tubulin was used as a protein loading control. *B*, Dose response to FasL-induced apoptosis in control cells (●) and Bcl-2 knockdown cells (○). Cells were incubated with the indicated concentrations of FasL for 24 h, after which apoptosis was measured by PI staining. *C*, Kinetics of caspase-3 activation following stimulation with 100 ng/ml FasL in control cells (●) and Bcl-2 knockdown cells (○) measured by intracellular staining with flow cytometry. *D*, Computer simulation of caspase-3 activation following a 10- or 100-fold decrease in Bcl-2 level.

Consideration of signaling network kinetics provided us a new approach to differentiate different interaction possibilities using relatively simple experimental methods. Bid, BAX, Bcl-x_L, and Bcl-2 (28–30) all have similar three-dimensional structures (28–30), and the structures of Bid and tBid are also similar to one another (28). This structural similarity is likely to confound other possible approaches. For example, we expect it would be difficult to differentiate the binding preference of Bcl-x_L/Bcl-2 for Bid, tBid, and Bax according to structure information, and coimmunoprecipitation experiments are also likely to give false results.

Because many parameters in the model are adjusted to fit the kinetics of two molecules, we performed additional simulations to make sure this conclusion is not limited to the specific parameter set used in our study. Specifically, we changed forward and reverse rate constants of Bcl-2 binding and the initial conditions of Bax and Bid individually. We find that, although the models with these different parameter values do not fit to experimental data as well as using the baseline values, whenever Bcl-2 is able to effectively block the mitochondrial pathway with at least one of the mechanisms, Bcl-2 binding to both Bax and tBid is the most efficient mechanism compared with Bcl-2 binding to Bax, Bid, or tBid alone.

In addition to the hypotheses tested above, there are other possible mechanisms by which Bcl-2 may block the mitochondrial pathway. For example, Bcl-2 may gate a mitochondrial pore independent of Bax/Bak to prevent the movement of material into and out of the mitochondria (31); Bcl-2 may compete with Bax/Bak binding to a third molecule to regulate the release of cytochrome *c*; or Bcl-2 may sequester some unknown caspase activator, as is seen in the analogous *Caenorhabditis elegans* system (32). These questions could be addressed in the future with a similar combined modeling and experimental approach when more data supporting these hypothetical mechanisms become available.

Sensitivity analysis and the nonlinearity of caspase-3 activation dependence on signal molecule levels

Sensitivity analysis of Bcl-2 using our computer simulation, and subsequently confirmed by our experimental data, demonstrates that caspase-3 activation is not linearly dependent on Bcl-2 expression level. Such nonlinearity can explain why the results of overexpression of a molecule are not necessarily opposite to those observed when a molecule is underexpressed. Interestingly, the asymmetric effect of Bcl-2 may allow therapies aimed at decreasing Bcl-2 to have a specific effect on tumor cells, thereby sparing healthy cells. According to the model analysis, the insensitivity of Jurkat cells to Bcl-2 down-regulation is due to the low level of endogenous Bcl-2, which does not block the type II pathway significantly. However, in many tumor cells, Bcl-2 is aberrantly upregulated to render tumor cells resistant to many apoptotic stimuli (22). In this case, decreasing Bcl-2 is equivalent to decreasing Bcl-2 from 10- or 100-fold of the baseline back to its original value, thus promoting cell death. At the same time, because normal and Jurkat cells both have low Bcl-2 levels, decreasing the level of Bcl-2 will have only a minimal effect on their apoptosis. Most

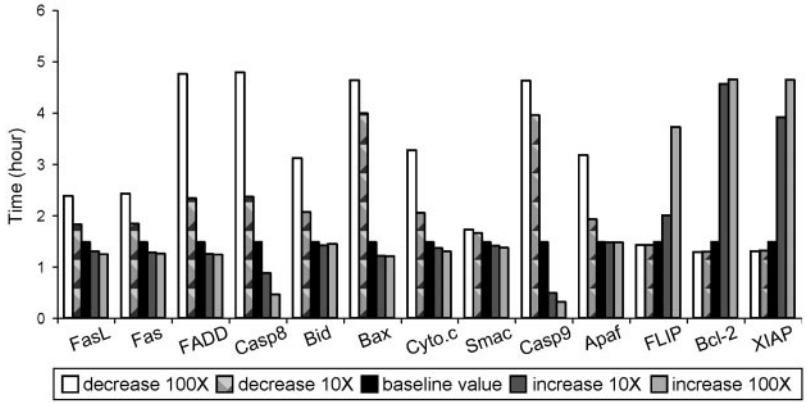

FIGURE 7. Sensitivity analysis for network model components. The expression level (initial condition for model calculations) of one component was changed for each simulation, while holding the others constant. Levels were changed one or two orders of magnitude in either direction from the baseline values. The half-time of caspase-3 activation is plotted to represent how fast caspase-3 becomes activated.

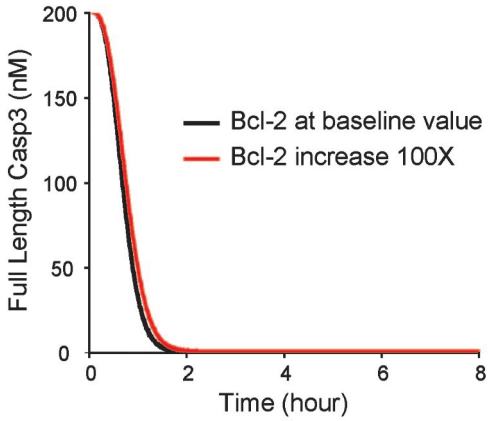

FIGURE 8. Conversion of the model to type I pathway dominant behavior. Computer simulation of caspase-3 activation with Bcl-2 either at the baseline level or 100 times the baseline level when caspase-8 level in the model was increased by 20 times.

anti-Bcl-2 drugs are being used to increase the efficiency of standard anticancer therapies. Although anti-Bcl-2 drugs will not affect the level of apoptosis in healthy cells caused by anticancer therapies, their coadministration should at least not aggravate this side effect.

Although the same sensitivity analysis, as described here for Bcl-2, could be done experimentally for all the molecules involved in the Fas signaling to identify potential drug targets, it would be extremely costly and time-consuming. Computer simulations using an experimentally validated model can help point out the most sensitive parts of a pathway, thereby identifying the key experiments most likely to generate interesting results.

The results of this sensitivity analysis explicitly depend on the baseline expression levels of all the molecules in the Fas signaling pathway. Because the baseline levels for some of the molecules might be different in different cell types, those other cell types may exhibit different sensitivities than those observed in our study.

Our sensitivity analysis of all the molecules involved in Fas signaling illustrates that the sensitivity of caspase-3 activation to the various molecules varies dramatically, and many signaling molecules have asymmetric effects on the signaling outcome. These results suggest that signaling cascades are highly nonlinear and nonintuitive. Consequently, understanding the kinetics of the overall signaling pathway using mathematical model is critical in understanding its regulation. More extensive discussions about the utility of models can be found elsewhere (26).

Limitations of the model and future improvements

Although our model describes many aspects of the Fas signaling system and, in particular, specific aspects of type II dominant signaling, there are limitations of the model. One discrepancy between our model and known biology is that, whereas the qualitative trends are similar, caspase-3 activation in the model is less sensitive to FasL concentration changes than has been reported experimentally. This may be due to the relatively simple ligand binding structure of the model and exclusion of endocytosis and receptor trafficking, both of which are known to modulate signaling dynamics in other receptor systems (e.g., epidermal growth factor receptor) (8). Extension of the model to address this issue is part of future model development.

More generally, there are various details in the Fas pathway that are not included in the current model. For example, we have not included the clustering of receptors on the cell membrane that occurs following Fas stimulation (33, 34), the phosphorylation-induced deactivation of Bcl-2 (35, 36), the regulation of the mitochondrial pathway by other Bcl-2 family members (27, 37), or the nonredundant functions of Bcl-2 and Bcl-xL (27, 30). Representing a simplified system at the beginning of a model's development follows a philosophy of question-oriented, iterative model development and validation. With this philosophy, each iteration of model development is focused on addressing particular research questions and includes careful and extensive validation. In this first iteration of our model, the focus is on reproducing only a few key system behaviors relevant to the problem of interest. The breadth and detail of its components and functions are limited to only those necessary to meet that goal. In future iterations, we must be cautious about expanding a model because it introduces more parameters and, if data are not available to assign them values, or at least constrain their values, they simply become free knobs for tuning the system that may provide too much flexibility to the model.

In summary, this study has demonstrated how the consideration of quantitative aspects and dynamics of a system, interpreted through a mathematical model and in collaboration with kinetics experiments, can provide additional understanding of a signaling system.

Acknowledgments

We thank John Albeck and Dr. Suzanne Gaudet for useful discussion and technical help. We thank Liming Yang for her help making Bcl-2 knockdown construct. We are also grateful for Rayka Yokoo's help with mathematical modeling.

Disclosures

The authors have no financial conflict of interest.

References

1. Rieux-Laucat, F., F. Le Deist, and A. Fischer. 2003. Autoimmune lymphoproliferative syndromes: genetic defects of apoptosis pathways. *Cell Death Differ.* 10: 124–133.
2. Igney, F. H., and P. H. Krammer. 2002. Death and anti-death: tumour resistance to apoptosis. *Nat. Rev. Cancer* 2: 277–288.
3. Ashkenazi, A., and V. M. Dixit. 1998. Death receptors: signaling and modulation. *Science* 281: 1305–1308.
4. Schmitz, I., S. Kirchhoff, and P. H. Krammer. 2000. Regulation of death receptor-mediated apoptosis pathways. *Int. J. Biochem. Cell Biol.* 32: 1123–1136.
5. Nagata, S. 1999. Fas ligand-induced apoptosis. *Annu. Rev. Genet.* 33: 29–55.
6. Scaffidi, C., S. Fulda, A. Srinivasan, C. Friesen, F. Li, K. J. Tomaselli, K. M. Debatin, P. H. Krammer, and M. E. Peter. 1998. Two CD95 (APO-1/Fas) signaling pathways. *EMBO J.* 17: 1675–1687.
7. Riedl, S. J., and Y. Shi. 2004. Molecular mechanisms of caspase regulation during apoptosis. *Nat. Rev. Mol. Cell Biol.* 5: 897–907.
8. Wiley, H. S., S. Y. Shvartsman, and D. A. Lauffenburger. 2003. Computational modeling of the EGF-receptor system: a paradigm for systems biology. *Trends Cell Biol.* 13: 43–50.
9. Wang, K., X. M. Yin, D. T. Chao, C. L. Milliman, and S. J. Korsmeyer. 1996. BID: a novel BH3 domain-only death agonist. *Genes Dev.* 10: 2859–2869.
10. Oltvai, Z. N., C. L. Milliman, and S. J. Korsmeyer. 1993. Bcl-2 heterodimerizes in vivo with a conserved homolog, Bax, that accelerates programmed cell death. *Cell* 74: 609–619.
11. Cheng, E. H., M. C. Wei, S. Weiler, R. A. Flavell, T. W. Mak, T. Lindsten, and S. J. Korsmeyer. 2001. BCL-2, BCL-X_L sequester BH3 domain-only molecules preventing BAX- and BAK-mediated mitochondrial apoptosis. *Mol. Cell* 8: 705–711.
12. Mikhailov, V., M. Mikhailova, D. J. Pulkrabek, Z. Dong, M. A. Venkatachalam, and P. Saikumar. 2001. Bcl-2 prevents Bax oligomerization in the mitochondrial outer membrane. *J. Biol. Chem.* 276: 18361–18364.
13. Kelly, E., A. Won, Y. Refaeli, and L. Van Parijs. 2002. IL-2 and related cytokines can promote T cell survival by activating AKT. *J. Immunol.* 168: 597–603.
14. Rubinson, D. A., C. P. Dillon, A. V. Kwiatkowski, C. Sievers, L. Yang, J. Kopinja, D. L. Rooney, M. M. Ihrig, M. T. McManus, F. B. Gertler, et al. 2003. A lentivirus-based system to functionally silence genes in primary mammalian cells, stem cells and transgenic mice by RNA interference. *Nat. Genet.* 33: 401–406.
15. Hickman, M. J., and L. D. Samson. 2004. Apoptotic signaling in response to a single type of DNA lesion, O^6-methylguanine. *Mol. Cell* 14: 105–116.
16. Siegel, R. M., J. K. Frederiksen, D. A. Zacharias, F. K. Chan, M. Johnson, D. Lynch, R. Y. Tsien, and M. J. Lenardo. 2000. Fas preassociation required for apoptosis signaling and dominant inhibition by pathogenic mutations. *Science* 288: 2354–2357.

17. Tanaka, M., T. Suda, T. Takahashi, and S. Nagata. 1995. Expression of the functional soluble form of human fas ligand in activated lymphocytes. *EMBO J.* 14: 1129–1135.
18. Kischkel, F. C., S. Hellbardt, I. Behrmann, M. Germer, M. Pawlita, P. H. Krammer, and M. E. Peter. 1995. Cytotoxicity-dependent APO-1 (Fas/CD95)-associated proteins form a death-inducing signaling complex (DISC) with the receptor. *EMBO J.* 14: 5579–5588.
19. Wei, M. C., W. X. Zong, E. H. Cheng, T. Lindsten, V. Panoutsakopoulou, A. J. Ross, K. A. Roth, G. R. MacGregor, C. B. Thompson, and S. J. Korsmeyer. 2001. Proapoptotic BAX and BAK: a requisite gateway to mitochondrial dysfunction and death. *Science* 292: 727–730.
20. Salvesen, G. S., and C. S. Duckett. 2002. IAP proteins: blocking the road to death's door. *Nat. Rev. Mol. Cell Biol.* 3: 401–410.
21. Armstrong, R. C., T. Aja, J. Xiang, S. Gaur, J. F. Krebs, K. Hoang, X. Bai, S. J. Korsmeyer, D. S. Karanewsky, L. C. Fritz, and K. J. Tomaselli. 1996. Fas-induced activation of the cell death-related protease CPP32 is inhibited by Bcl-2 and by ICE family protease inhibitors. *J. Biol. Chem.* 271: 16850–16855.
22. Reed, J. C., T. Miyashita, S. Takayama, H. G. Wang, T. Sato, S. Krajewski, C. Aime-Sempe, S. Bodrug, S. Kitada, and M. Hanada. 1996. BCL-2 family proteins: regulators of cell death involved in the pathogenesis of cancer and resistance to therapy. *J. Cell. Biochem.* 60: 23–32.
23. Klasa, R. J., A. M. Gillum, R. E. Klem, and S. R. Frankel. 2002. Oblimersen Bcl-2 antisense: facilitating apoptosis in anticancer treatment. *Antisense Nucleic Acid Drug Dev.* 12: 193–213.
24. Barnhart, B. C., E. C. Alappat, and M. E. Peter. 2003. The CD95 type I/type II model. *Semin. Immunol.* 15: 185–193.
25. Fussenegger, M., J. E. Bailey, and J. Varner. 2000. A mathematical model of caspase function in apoptosis. *Nat. Biotechnol.* 18: 768–774.
26. Bentele, M., I. Lavrik, M. Ulrich, S. Stosser, D. W. Heermann, H. Kalthoff, P. H. Krammer, and R. Eils. 2004. Mathematical modeling reveals threshold mechanism in CD95-induced apoptosis. *J. Cell Biol.* 166: 839–851.
27. Cory, S., and J. M. Adams. 2002. The Bcl2 family: regulators of the cellular life-or-death switch. *Nat. Rev. Cancer* 2: 647–656.
28. Chou, J. J., H. Li, G. S. Salvesen, J. Yuan, and G. Wagner. 1999. Solution structure of BID, an intracellular amplifier of apoptotic signaling. *Cell* 96: 615–624.
29. McDonnell, J. M., D. Fushman, C. L. Milliman, S. J. Korsmeyer, and D. Cowburn. 1999. Solution structure of the proapoptotic molecule BID: a structural basis for apoptotic agonists and antagonists. *Cell* 96: 625–634.
30. Petros, A. M., A. Medek, D. G. Nettesheim, D. H. Kim, H. S. Yoon, K. Swift, E. D. Matayoshi, T. Oltersdorf, and S. W. Fesik. 2001. Solution structure of the antiapoptotic protein bcl-2. *Proc. Natl. Acad. Sci. USA* 98: 3012–3017.
31. Tsujimoto, Y., and S. Shimizu. 2000. VDAC regulation by the Bcl-2 family of proteins. *Cell Death Differ.* 7: 1174–1181.
32. Ottilie, S., Y. Wang, S. Banks, J. Chang, N. J. Vigna, S. Weeks, R. C. Armstrong, L. C. Fritz, and T. Oltersdorf. 1997. Mutational analysis of the interacting cell death regulators CED-9 and CED-4. *Cell Death Differ.* 4: 526–533.
33. Siegel, R. M., J. R. Muppidi, M. Sarker, A. Lobito, M. Jen, D. Martin, S. E. Straus, and M. J. Lenardo. 2004. SPOTS: signaling protein oligomeric transduction structures are early mediators of death receptor-induced apoptosis at the plasma membrane. *J. Cell Biol.* 167: 735–744.
34. Cremesti, A., F. Paris, H. Grassme, N. Holler, J. Tschopp, Z. Fuks, E. Gulbins, and R. Kolesnick. 2001. Ceramide enables fas to cap and kill. *J. Biol. Chem.* 276: 23954–23961.
35. Yamamoto, K., H. Ichijo, and S. J. Korsmeyer. 1999. BCL-2 is phosphorylated and inactivated by an ASK1/Jun N-terminal protein kinase pathway normally activated at G_2/M. *Mol. Cell. Biol.* 19: 8469–8478.
36. Scaffidi, C., J. Volkland, I. Blomberg, I. Hoffmann, P. H. Krammer, and M. E. Peter. 2000. Phosphorylation of FADD/MORT1 at serine 194 and association with a 70-kDa cell cycle-regulated protein kinase. *J. Immunol.* 164: 1236–1242.
37. Tsujimoto, Y. 2003. Cell death regulation by the Bcl-2 protein family in the mitochondria. *J. Cell. Physiol.* 195: 158–167.
38. Goltsev, Y. V., A. V. Kovalenko, E. Arnold, E. E. Varfolomeev, V. M. Brodianskii, and D. Wallach. 1997. CASH, a novel caspase homologue with death effector domains. *J. Biol. Chem.* 272: 19641–19644.
39. Pitti, R. M., S. A. Marsters, D. A. Lawrence, M. Roy, F. C. Kischkel, P. Dowd, A. Huang, C. J. Donahue, S. W. Sherwood, D. T. Baldwin, et al. 1998. Genomic amplification of a decoy receptor for Fas ligand in lung and colon cancer. *Nature* 396: 699–703.
40. Huang, Y., R. L. Rich, D. G. Myszka, and H. Wu. 2003. Requirement of both the second and third BIR domains for the relief of X-linked inhibitor of apoptosis protein (XIAP)-mediated caspase inhibition by Smac. *J. Biol. Chem.* 278: 49517–49522.
41. Renatus, M., H. R. Stennicke, F. L. Scott, R. C. Liddington, and G. S. Salvesen. 2001. Dimer formation drives the activation of the cell death protease caspase 9. *Proc. Natl. Acad. Sci. USA* 98: 14250–14255.
42. Boatright, K. M., M. Renatus, F. L. Scott, S. Sperandio, H. Shin, I. M. Pedersen, J. E. Ricci, W. A. Edris, D. P. Sutherlin, D. R. Green, and G. S. Salvesen. 2003. A unified model for apical caspase activation. *Mol. Cell* 11: 529–541.
43. Riedl, S. J., M. Renatus, R. Schwarzenbacher, Q. Zhou, C. Sun, S. W. Fesik, R. C. Liddington, and G. S. Salvesen. 2001. Structural basis for the inhibition of caspase-3 by XIAP. *Cell* 104: 791–800.
44. Letai, A., M. C. Bassik, L. D. Walensky, M. D. Sorcinelli, S. Weiler, and S. J. Korsmeyer. 2002. Distinct BH3 domains either sensitize or activate mitochondrial apoptosis, serving as prototype cancer therapeutics. *Cancer Cell* 2: 183–192.
45. Sun, X. M., S. B. Bratton, M. Butterworth, M. MacFarlane, and G. M. Cohen. 2002. Bcl-2 and Bcl-x_L inhibit CD95-mediated apoptosis by preventing mitochondrial release of Smac/DIABLO and subsequent inactivation of X-linked inhibitor-of-apoptosis protein. *J. Biol. Chem.* 277: 11345–11351.